Chapter 10
Geological Evolution of the Himalayan Mountains

A. K. Jain

Abstract The Indian continental lithospheric (ICL) Plate did not collide with Asia, initially due to the presence of vast Neo-Tethyan Ocean. Instead, the ICL first subducted beneath the Trans-Himalayan Ladakh magmatic arc at ~58 Ma to produce the ultrahigh-pressure (UHP) metamorphosed Tso Morari Crystallines (TMC). The Himalaya first emerged from this deeply subducted terrane between 53 and 50 Ma, followed by sequential subduction and imbrications of the ICL. It was repeatedly metamorphosed during ~45–35 and ~25–15 Ma and had undergone episodic exhumation during rise of the Himalaya since 45 Ma, whose erosion brought huge sediments in the Cenozoic Himalayan foreland basin.

Sub-horizontal subduction of the Indian Plate beneath the Himalaya caused accretion/imbrication of the upper crust by ongoing northward episodic push, which caused southward-directed thrusts. True signature of continental collision can only be identified along the Bangong-Nujiang Suture (BNS) Zone in Central Tibet with opposite downward convergence of the India and Asian Plates.

Keywords India-Asia convergence · Himalaya · Geometry Indian Plate Continental subduction vs. collision

10.1 Introduction

Paleogeographic reconstructions of the India-Asia domains during the Mesozoic postulate that the Tethyan Ocean separated the northern parts of the Indian continental lithosphere (ICL) from the southern Asian Plate (Stampfli and Borel 2002). These regions now constitute the Himalaya, Trans-Himalayan Ladakh-Karakoram Mountains and Tibet Plateau. As the Indian Plate converged anti-clockwise and northwards towards Asia, the Neo-Tethyan oceanic floor underwent intra-oceanic subduction to produce the Shyok-Dras Volcanic Arc (Searle et al. 1987; Thakur 1993; Rolland et al. 2000; Jain and Singh 2009; Copley et al. 2010). Between this

A. K. Jain (✉)
CSIR-Central Building Research Institute, Roorkee, India

N. Gupta, S. K. Tandon (eds.), *Geodynamics of the Indian Plate*,
Springer Geology, https://doi.org/10.1007/978-3-030-15989-4_10

arc and Asian Plate, a thick Paleo-Mesozoic Karakoram sedimentary sequence was deposited on its southern margin. This ocean closed along the Shyok suture zone (SSZ) in the north and subsequently along the Indus-Tsangpo Suture Zones (ITSZ) in the south; two sutures demarcate contact between these plates (Fig. 10.1). These sutures preserve evidences of (1) initial Late Mesozoic subduction of the Neo-Tethys oceanic lithosphere along the SSZ during the Early Cretaceous-Lower Eocene with intervening intra-oceanic Shyok-Dras Volcanic Arc, (2) emplacement of the younger calc-alkaline Trans-Himalayan plutons and (3) final closure of the Neo-Tethys along the ITSZ (Honegger et al. 1982; Searle et al. 1987; Hodges 2000; Rolland et al. 2000; Yin 2006; Jain and Singh 2008, 2009).

The ICL, its Proterozoic-Paleozoic supracrustals and Paleo-Mesozoic Tethyan sedimentary cover were remobilized south of the ITSZ and underwent Cenozoic deformation and metamorphism. It formed the Himalayan Metamorphic Belt (HMB) whose leading edge in the Tso Morari suffered ultrahigh-pressure (UHP) metamorphism at 53.3 ± 0.7 Ma at >120 km depth beneath the Trans-Himalaya (Leech et al. 2005). Various thrusts such as the Main Central Thrust (MCT) and Main Boundary Thrust (MBT) caused extensive crustal shortening during the Himalayan tectonics (Fig. 10.1; Thakur 1993; Yin 2006).

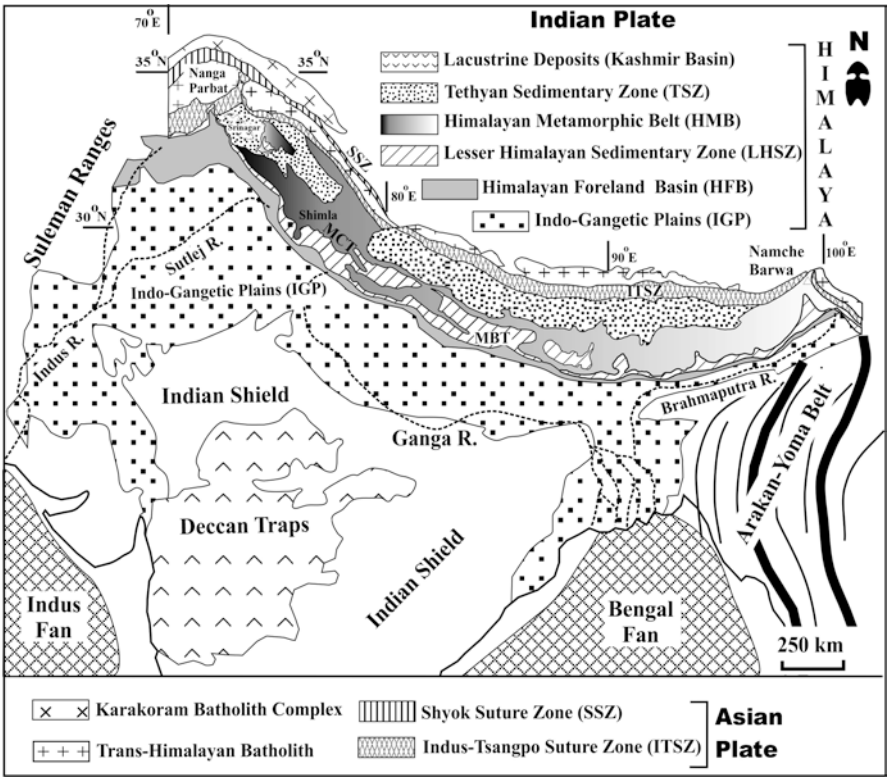

Fig. 10.1 Simplified regional geological map of the Himalaya and adjoining mountains in the plate tectonic framework. Also shown are the Cenozoic Sub-Himalayan foreland basin (HFB), Recent Indo-Gangetic Plains and Indus-Bengal Fans, receiving sediments from the eroding mountains. *SSZ* Shyok suture zone, *ITSZ* Indus Tsangpo suture zone, *MCT* main central thrust, *MBT* main boundary thrust. (Compiled from published data)

Two contrasting hypotheses attempted to explain the geological evolution of the Himalaya: (1) continental lithospheric collision between the Indian and Asian Plates along the ITSZ (Dewey and Bird 1970; Thakur 1993; Hodges 2000; Searle et al. 1987; Jain et al. 2002; Yin 2006; Valdiya 2016) and (2) continental lithospheric subduction beneath the Himalaya and Tibet till Kunlun (Argand 1924; Powell and Conaghan 1973, 1975; Seeber et al. 1981; Ni and Barazangi 1984; Zhao et al. 1993; Nelson et al. 1996; Nábělek et al. 2009; Jain 2014; Jain 2017; Guo et al. 2017). This chapter highlights geological and geophysical evidences to postulate that continental lithospheric subduction of the Indian Plate and sequential imbrication of the overriding sequences are the dominant geological mechanisms in the evolution of the Himalaya during the Cenozoic.

10.2 Himalayan Orogen

Almost continuous litho-tectonic units characterize the southward Cenozoic convergence in the Himalayan orogen (Fig. 10.2). These units are tectonically juxtaposed from south to north: (1) the Indo-Gangetic Plains against the Sub-Himalayan (SH) belt along the Himalayan Frontal Thrust (HFT), (2) the SH belt against the Lesser Himalaya (LH) sedimentary belt along the Main Boundary Thrust (MBT), (3) the LH Belt against the HMB along the Main Central Thrust Zone (MCTZ) and (4) the HMB against the Tethyan Himalayan Sequence (THS) along the South Tibetan Detachment Zone (STDS) (Heim and Gansser 1939; Thakur 1993; Hodges 2000; Yin 2006; Jain et al. 2014; Valdiya 2016).

10.2.1 Cenozoic Himalayan Foreland Basin (HFB)

The HFB is an elongated asymmetrical basin between the Himalayan Frontal Thrust (HFT) towards south and the MBT in the north, whose sediment pile extends into the Indo-Gangetic Plains (IGP), where it overlaps the peripheral bulge of the Indian Craton (Tandon 1991; Singh 1999; Kumar et al. 2009). Many transverse basement ridges dissect the HFB into several sub-basins and control their sedimentation patterns and tectonics. It evolved with widespread Paleocene-Middle Eocene marine transgression, covering parts of the Lesser Himalaya. This basin predominantly accumulated fluvial sediments, which were deposited by southward-flowing river systems from the rising Himalaya (Srikantia and Bhargava 1998). Four stratigraphic units characterize this belt (Fig. 10.3).

10.2.1.1 Subathu Formation

The oldest marine Subathu Formation (Paleocene-Middle Eocene in age) unconformably overlies the basement and contains silicified limestone clasts and bauxite at the base, coaly/carbonaceous shale and fossiliferous grey-green

Fig. 10.2 Geological map of the NW Himalaya, Trans-Himalaya and Karakoram Mountains showing their main tectonic units. See text for details. (Map compiled after author's extensive traverses, published literature and Jain and Singh 2009)

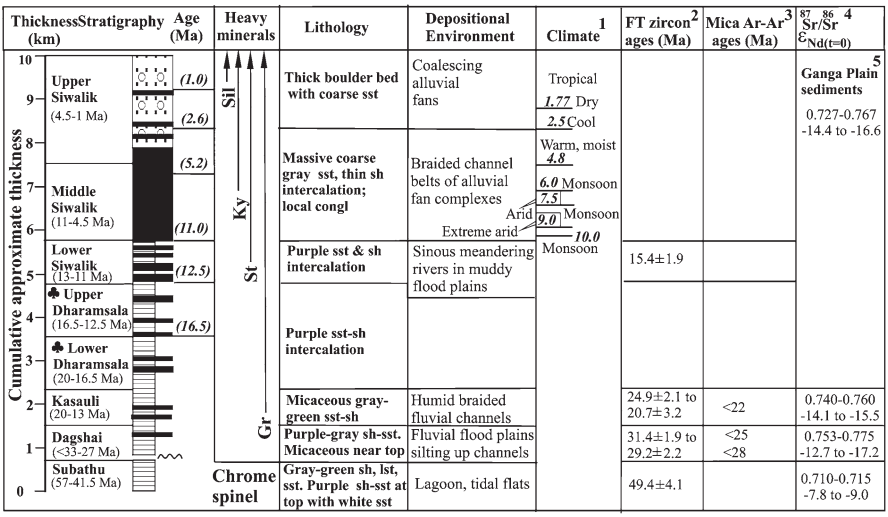

♣ Stratigraphic equivalents of the Kasauli Fm. (Himachal). 1-Kumar et al. (2011). 2-Jain et al. (1999). 3-Najman (2006). 4. Najman et al. (2000). 5-Rahaman et al. (2009)

Fig. 10.3 Generalized stratigraphy of the Cenozoic HFB in Himachal Pradesh (Jain et al. 2009; Clift 2017). (Data source: (1) Kumar et al. (2009) for climate, (2) Jain et al. (2009) for detrital FT zircon ages, (3) Najman (2006) for detrital mica $^{40}Ar/^{39}Ar$ ages, (4, 5) Najman et al. (2000) and Rahaman et al. (2009) for whole-rock $^{87}Sr/^{86}Sr$ and $\varepsilon_{Nd(t=0)}$ isotope characters)

shale-siltstone and limestone-sandstone, which grade into variegated purple siltstone-shale (Passage bed) and, in turn, by white sandstone (Bhatia and Bhargava 2006). It was deposited in euxinic-evaporitic lagoons and shallow tidal sea. It is marked by relatively high $\varepsilon_{Nd(t=0)}$ values (~−7.8 to −9) and low $^{87}Sr/^{86}Sr$ ratios (~0.710–0.715), with detritus sourced ffrom the proto-Himalaya and ITSZ (Najman et al. 2000).

10.2.1.2 Dagshai Formation

The overlying unfossiliferous Dagshai Formation (Dharamsala Formation) contains reddish mudstone-siltstone-sandstone alternations. Precise contact relationships between the Subathu and Dagshai Formations are debated since a transition was postulated from marine to fluvial environment (Bhatia and Bhargava 2006), in contrast to an unconformity with a hiatus of ~10 my to <3 my. Age of the Dagshai Formation is also uncertain: (1) 35.5 ± 6.7 Ma, between <28 and 25 Ma from the $^{40}Ar/^{39}Ar$ detrital micas, or (2) base younger than 31 ± 2 Ma from detrital zircon fission-track (ZFT) ages or (3) 35.5 Ma, magnetostratigraphically (Najman 2006; Jain et al. 2009). The $\varepsilon_{Nd(t=0)}$ and $^{87}Sr/^{86}Sr$ isotopic values range between ~−12.7 to −17.2 and ~0.753 to 0.775, respectively (Najman et al. 2000), indicating sources like medium-grade metamorphosed HHC.

10.2.1.3 Kasauli Formation

The overlying Kasauli Formation contains alternating grey-green sandstone and siltstone-mudstone, which were deposited by migratory braided river system under humid climate. It possesses more metamorphic fragments than older formations, with isotopic characters like the Dagshais. Age of this formation remains uncertain: Lower Miocene (23–16 Ma) from floral and mammal remains, <28 to 22 Ma from $^{40}Ar/^{39}Ar$ detrital white mica and 24.9 ± 2.1 to 20.7 ± 3.2 Ma from youngest ZFT peak for the uppermost part (Jain et al. 2009).

10.2.1.4 Siwalik Group

Over 6-km-thick Miocene-Pleistocene sequences in the HFB characterize this group, which was deposited by southerly flowing fluvial system (Kumar et al. 2009). The Lower Siwalik Subgroup of interbedded coarse purple-grey sandstone-brown shale was deposited by highly sinuous meandering rivers in broad muddy flood plains (Singh 1999). Detritus was mainly derived from low-medium-grade metamorphosed Himalayan sources between <13 and 9 Ma (cf. Clift 2017). About 2.5-km-thick Middle Siwalik Subgroup of greyish, mica-rich medium to coarse multi-storied sandstone-siltstone-overbank mudstone were deposited by braided rivers with alluvial fan complexes between 9 and 4.5 Ma. The Upper Siwalik Subgroup of ~2.5-km-thick conglomerate-sandstone-mudstone was laid down into coalescing alluvial fans between 4.5 and 1 Ma.

Since the HFB detritus was synchronously derived from the Himalaya, it provides an invaluable clue for cooling and exhumation of adjacent rising hinterlands. Detrital $^{40}Ar/^{39}Ar$ muscovite and ZFT youngest peaks become younger eastwards from 25–20 to 10–8 Ma; this trend is consistent with an eastward-migrating pulse of hinterland cooling (Clift 2017; Webb et al. 2017).

10.2.1.5 Indo-Gangetic Plains

The largest active foreland basin—the Indo-Gangetic Plains (IGP)—Brahmaputra and Bengal Basins along southern margin of the Himalaya accumulates enormous eroded sediments and dissolved materials by huge rivers, which also carry these into mega-fans of the Bay of Bengal-Arabian Sea. Many Archean basement ridges, faults and unevenly overlying Vindhyan Group extend northwards and dissect these basins into deeper depocentres, where sediments (the Siwaliks) accumulate to nearly 6.0 km thick near the Himalayan foothills (see Singh 1999; Clift 2017 for details).

A 50 m sediment core at Kanpur near Ganga River records a 100 m uninterrupted flood plain deposit, having two pronounced excursions at ca. 70 and 20 ka and variations in $^{87}Sr/^{86}Sr$ ratio and $\varepsilon_{Nd(0)}$ values from 0.727 to 0.767 and −14.4 to −16.6, respectively (Rahaman et al. 2009). These coincide with decreased monsoon precipitation and an increase in glacial cover, which caused lower sediment supply from the Higher Himalaya.

10.2.2 Lesser Himalayan (LH) Sedimentary Belt

Two sedimentary belts characterize this domain between the MBT and the MCT (Table 10.1): (1) southern Neoproterozoic-Early-Paleozoic Outer Lesser Himalayan (OLH) sedimentary belt of the Shimla-Jaunsar-Blaini-Krol-Tal Groups and Subathu Formation between the MBT and Tons Thrust (TT)/North Almora Thrust (NAT) and (2) northern Inner Lesser Himalayan (ILH) sedimentary belt of the Paleoproterozoic Shali-Rautgara-Gangolihat-Deoban-Berinag-Kuncha-Daling-Shumar Groups between the TT/NAT and MCT (Valdiya 1980; Jain et al. 2014). The ILH is exposed in the Kishtwar and Kulu-Rampur windows in Himachal, Ghuttu window in Garhwal, Arun window in Nepal, Ranjit window in Sikkim, Kuru Chu window in Bhutan and Nacho-Menga windows in Arunachal.

10.2.2.1 The Outer Lesser Himalayan (oLH) Sedimentary Belt

In this belt, oldest Shimla Group (Morar-Chakrata-Dharasu-Srinagar-Pauri Groups) contains intercalated protoquartzite-slate-limestone-dolomite sequences (Fig. 10.2; Srikantia and Bhargava 1998), which were deposited as flysch turbidite, tidal flat complex or prograding muddy delta sequence.

Further south, within the Krol Belt, oldest Neoproterozoic Jaunsar Group contains the Mandhali Formation (conglomerate-limestone-carbonaceous-slate-phyllite), the Chandpur Formation (alternating phyllite-siltstone-metavolcanics) and the Nagthat Formation (quartz arenite-slate). The overlying Blaini-Krol-Tal Groups contain typical Marinoan Blaini diamictite and associated sandstone-shale-pink limestone, which were deposited under glaciomarine conditions. The overlying Ediacaran Infra Krol Formation of alternating greywacke-siltstone-shale is succeeded by thick greyish carbonates of the Krol Group with five formations of sandstone-shale-limestone and was deposited under tidal to intertidal environments. The overlying Lower Cambrian Tal Group is phosphorite-chert-shale-greywacke in the basal parts and thick quartzite in the upper parts. The lower Paleocene Subathu Formation unconformably overlies this belt with an intervening arenaceous shelly limestone of Upper Cretaceous age.

Detrital zircon population from the Krol Belt has the youngest U-Pb peak of 0.95 Ga in the Mandhali Formation and becomes gradually younger in the Chandpur Formation (~0.88 Ga) and the Nagthat Formation (~0.82 Ga); $\varepsilon_{Nd(t=0)}$ values range between −14 and −19. This peak becomes still younger with the incoming of 0.70–0.525 Ga grains in the Blaini diamictite and trilobite-bearing Late Early Cambrian Lower Tal, respectively (Hofmann et al. 2011; Myrow et al. 2003).

10.2.2.2 Inner Lesser Himalayan (ILH) Sedimentary Belt

In Jammu-Kashmir and southern Himachal Pradesh, outermost frontal Paleoproterozoic ILH Shali Belt contains quartzite-shale (Sundernagar Formation), mafic volcanics-slate (Mandi-Darla volcanics) and salt-marls-shale-quartzite-dolomite (Shali Group). This imbricated belt is thrust southwestward over the SH belt in Punjab re-entrant along the MBT (Table 10.1; Srikantia and Bhargava 1998). It contains the Tatapani limestone and Deoban Group carbonates within the Kulu-Rampur and other smaller windows along the Sutlej-Tons valleys beneath the Jutogh Nappe and MCT zone (Fig. 10.2).

Further east, an extensive ILH Paleoproterozoic sedimentary sequence is developed beneath the overthrust metamorphic nappes between the NAT and MCT in Uttarakhand. The oldest Rautgara Formation starts with subgreywacke-slate-conglomerate-mafic flows (Valdiya 1980) and imperceptibly grades into the overlying stromatolite-bearing dolomitic limestone slate of the Gangolihat Formation and mature quartz arenite-mafic flows of the Berinag/Garhwal Groups.

Detrital U-Pb zircon ages from the ILH sequences—Rampur-Bhowali-Rautgara-Gangolihat-Berinag-Deoban-Damtha, Daling Group in Sikkim and Shumar Group in Bhutan including metabasalt-metarhyodacite flows reveal youngest peak between 2.0 and 1.8 Ga and $\varepsilon_{Nd(0)}$ values between −27.7 and −23.4 (Mandal et al. 2016). Thus, deposition in this belt terminated at ~1.9–1.8 Ga and undisputedly reveal a major stratigraphic break of nearly 1.0–0.9 Ga duration between these belts.

Table 10.1 Composite tectonostratigraphy of the Lesser Himalayan (LH) sequence, Himachal, Uttarakhand

Belts		Group	Formation	Lithology	U-Pb Zr age (Ga)[a]	$\varepsilon_{Nd(t=0)}$
Garhwal Nappe		Amri/Bijni		Phy-sch-qz		
Garhwal Thrust						
Upper Cretaceous-Eocene			Subathu Fm	Ss-sh-ls		
			SingtaliLs	Arenool ls		
Unconformity (Span, ~0.4 Ga)						
Cambrian		Tal Group	Upper Tal Fm	Qtz aren		
			Lower Tal Fm	Phos-Cht-Sh	0.525	−17.65
Neoproterozoic	Outer Lesser Himalaya (OLH)	Krol Group	Krol-E Fm	Gry Ls Frac		
			Krol-D Fm	Cht-Ls-Sh		
			Krol-C Fm	Bl Gr Ls, Frac		
			Krol-B Fm	Purp Gn Sh-Ls		
			Krol-A Fm	Dol Ls-Cht-Sl		
			Infra-Krol Fm	Sh-Sl-Qtz		
		Blain Group	Limestone-Sh Diamictite Quartzite Diamictite	Pk Microxln-Ls Gr Gn Diamict-Sh Qtzt Diamict	0.70	
		Jaunsar Group	Nagthat Fm	Wh Sst-Ark-Qtzt Cgl-Sltst	0.82	−14 to −19
			Chandpur Fm	Gn-Qtzt-Phyl	0.88	
			Mandhali Fm	Qtzt-Ls-Mbl-Cgl-Sltst-Phyl	0.95	
		Simla/Chakrata/Dharasu/ Srinagar/Pauri Group	Sanjaui Fm	Cgl-Sh-Qtzt-Gwke-Sh-Slt-St		
			Chaosa Fm	Gn-Purpsh-Slt-St-Gwke		
			Kunihar Fm	Ls-Dol-Sh-Slt-St		
			Basantpur Fm	Wh Qtz-Cgl-Sh-Slt-St-Ls		

Unconformity (Span, ~1.0 Ga)						
Paleoproterozoic	Inner Lesser Himalaya (ILH)	Garhwal/Pithoragarh	Berinag Fm (Gamri, Rampur, Manikaran)	Pk-Wh Qz Aren-Qz Sch-Amphi	2.0–1.7	−27.7 to −23.4
			Gangolihat/Deoban/Shali/ Tatapani Gr	Ma gr Dol-Ls-Stromlt Ls-Slt		
			Rautgara Fm	Gwke-Sl-Amph		
		Base not exposed				

Abbreviations: *Bl* blue, *Gn* green, *Gry* grey, *Pk* pink, *Purp* purple, *Wh* white, *Fm* formation, *Frac* fracture, *Microxln* microcrystalline, *Aren* arenite, *Ark* arkose, *Cgl* conglomerate, *Cht* chert, *Dol* dolomite, *Gr* group, *Gwke* greywacke, *Ls* limestone, *Ma* massive, *Mb* marble, *Mirostyl* microcrystalline, *Ool* oolitic, *Ss* sandstone, *Sch* schist, *Sh* shale

[a]Maximum depositional age

10.2.3 Himalayan Metamorphic Belt (HMB)

Folded thrust nappe of the Himalayan Metamorphic Belt (HMB) extensively covers the LH belts and is exposed into the Lesser Himalayan Crystallines (LHC), Higher Himalayan Crystallines (HHC) and the Tso Morari Crystallines (TMC) from south to the north (Fig. 10.2). An extensional Zanskar Shear Zone (ZSZ)/South Tibetan Detachment System (STDS) separate this belt from the THS.

10.2.3.1 LHC Belt

Numerous klippen of low-medium-grade metamorphosed LHC—the Salkhala Nappe, Garhwal and Almora Nappe, etc. contain highly deformed alternating phyllite and schist. The lowermost Ramgarh Nappe of mylonite orthogneiss (~ca. 1.85 Ga), belonging to the MCTZ, is overlain by quartzite-phyllite of the Nathuakhan Formation, having ~0.80 Ga detrital zircons (Mandal et al. 2015). The Almora Nappe overrides this unit with mylonitized granite gneiss (~1.85 Ga) along the base and garnetiferous quartzite-schist alternations with 0.85–0.58 Ga youngest detrital zircons and 0.55 Ga intrusive granitoids (Mandal et al. 2015).

10.2.3.2 HHC Belt

Located between the MCT and STDS, this belt is comprised of two sub-units in the Greater Himalaya: (1) a lower *Munsiari Group* (Main Central Thrust Zone (MCTZ)/Lesser Himalayan Crystallines (LHC)/Kulu-Bajura Nappe) and (2) an upper *Vaikrita Group/Great Himalayan Sequence (GHS) belt/Tibetan Slab*. The Munsiari Group contains intensely mylonitized biotite paragneiss, garnetiferous mica schist-phyllonite-amphibolites-quartzite and imbricated megacrystic granite mylonite. It is regionally thrust over the ILH along the MCT sensu stricto/Munsiari Thrust (MT) (Heim and Gansser 1939; Valdiya 1980). North-dipping ~15-km-thick GHS slab contains garnet-kyanite-biotite-muscovite ± kyanite ± sillimanite schist/gneiss, calc-silicates, garnet-amphibolite, migmatite and leucogranite; slab is bounded by the VT and STDS along the lower and upper margins, respectively (Jain et al. 2014).

Low- to medium-grade Jutogh Nappe, sandwiched between the OLH/ILH and the MCTZ, joins the basal parts of the THS in parts of Pabbar-Satluj-Beas valleys (Bhargava and Srikantia 2014).

U-Pb zircon ages from the Munsiari Group mylonite range between 1.9 and 1.75 Ga, while the overlying GHS possesses youngest detrital zircons of ~0.85 Ga; their $\varepsilon_{Nd(t=0)}$ values are around −25.0 and −17.0, respectively. Based on these distinct and regional isotopic characters of the GHS, its lowermost tectonic contact—the Vaikrita Thrust/Main Central Thrust (MCT)—either with the LH belt or the Munsiari/Ramgarh Group defines the terrane boundary.

The HHC is intensely sheared with top-to-the-south sense of ductile shearing and superposed top-to-the-north shearing near the STDS. An early prograde M1 regional metamorphism characterizes this belt at 45–35 Ma, 8–9 kb and 600–700 °C and a younger M2 event at 25–15 Ma, 6–8 kb and 500–750 °C (Hodges 2000; Yin 2006; Kohn 2014). Intense ductile shearing caused inverted metamorphism in this belt along with melting, cooling and exhumation since Miocene (Jain and Manickavasagam 1993).

10.2.3.3 TMC Belt

The TMC is comprised of ~100 × 50-km-long and NW-SE trending dome of quartzo-feldspathic gneiss, metamorphics and Paleozoic granitoids (Puga, Tanglang La, Polokongka La/Rupshu Granite, respectively) and small eclogite and garnet amphibolite bodies (Fig. 10.2; Thakur 1993; Jain et al. 2003; Leech et al. 2005). It is a UHP eclogite-gneiss-greenschist complex in southeastern Ladakh beneath the THS cover to the south of the ITSZ. Presence of coesite-bearing eclogite within the TMC and Kaghan (Pakistan) provides undisputed evidence that leading edge of the ICL subducted beneath the ITSZ to ~120 km depth in Early Eocene (Leech et al. 2005; Guillot et al. 2008).

The TMC attained peak P-T conditions for the UHP eclogite-gneiss at 750–850 °C and 2.7–3.9 GPa at ~55 Ma (de Sigoyer et al. 2000) and retrogressed to HP eclogite facies (600 °C, 2.0 GPa), amphibolite facies (600 °C, 1.3 GPa) and greenschist facies (350 °C, 0.4 GPa) and finally exhumed to the surface (Guillot et al. 1997). U-Pb SHRIMP zircon dates from the TMC pinpoint precise ages of peak UHP metamorphism (53.3 ± 0.7 Ma), HP metamorphism (50.0 ± 0.6 Ma) and amphibolite metamorphism (47.5 ± 0.5 Ma). ~30 Ma age of $^{40}Ar/^{39}Ar$ muscovite and biotite records last stage greenschist metamorphism (Leech et al. 2005, 2007).

10.2.4 Tethyan Himalayan Sequence (THS)

The THS was developed on northern passive margin of the Paleoproterozoic-Neoproterozoic Indian Plate during Cambrian to Paleogene/Lower Eocene with most representative sequences in Spiti (Table 10.2; Bhargava 2008). The THS commenced with eruptions of the Khewra Traps and Singhi bimodal volcanics in Salt Range and Bhutan, respectively, in a rift basin. The Cambrian sequence (Kunzum La Formation) has remarkable lithological similarity from Kashmir to Bhutan and deposited in subtidal to locally supratidal environments, except in Nepal. This sedimentation ranged up to Middle Cambrian; a part of Late Cambrian is preserved only in Kashmir and Bhutan. A widespread regression commenced in Late Cambrian and culminated in Early Ordovician due to the Kurgiakh Orogeny.

The Kurgiakh Orogeny caused the uplift and erosion of highlands and contributed conglomerate at the base of Ordovician. The Early Ordovician (Thango

Table 10.2 Tethyan stratigraphic sequence, Spiti in Himachal (Bhargava 2008)

Age	Formation/group	Lithology	Depositional environments
Eocene	Chikkim Fm	Ls-Sh	Shelf edge
Cretaceous	Giumal Fm	Ss	Shallow-?proximal turbidite
Jurassic	Spiti Fm	Sh-Sch	Mid-shelf
Disconformity			
Triassic	Lilang Super Gr	Ls-Sh-Ss-Sch	Shallow to deeper marine
Disconformity			
Permian	Kuling Gr	Ss-Sch-Sh	Mid-shelf
Late Carboniferous	GanmachidamFm	Cgl-Ss-Sh	Upper shore face culminating at beach
Early-Late Carboniferous	Po Fm	Ss-Sh-Sch	Mid-shelf culminating in upper shore face
Mid Devonian-Early Carboniferous	Lipak Fm	Ls-Ss-Sh-Sch	Subtidal to intertidal sea and restricted platform environment
Early(?)-Mid-Devonian	Muth Fm	Ss	Beach to barrier island
Disconformity			
Late Ordovician-Mid (?)-Silurian	Takche Fm	Ls-Sch-Ss-Sh	Subtidal-intertidal interface, with periodic storm episodes
Early Ordovician	Thango Fm	Ss-Sch-Sh-Cgl	Transgressive beach, tidal
Angular Unconformity			
Early-Late Cambrian	Kunzum La (Parahio) Fm	Ss-Sh-Sch-Ls	Subtidal-locally supratidal in upper part

Abbreviations: *Fm* formation, *Cgl* conglomerate, *Gr* group, *Ls* limestone, *Mirostyl* microcrystalline, *Ss* sandstone, *Sch* schist, *Sh* shale

Formation) is mainly arenaceous with a basal conglomerate up to Nepal, while in Bhutan sedimentation seems to have commenced in Late Ordovician. During this period, carbonates (Takche/Shiala/Yong Formations) have conspicuous build-ups in Kashmir-Spiti-Kinnaur-Garhwal-Bhutan and imperceptibly pass into another carbonate succession in Early Silurian, which may be extending into the Wenlock.

Regression in the Wenlock caused disconformity between the Early Silurian and Early Devonian; this break is more pronounced in western Spiti-Lahaul-Zanskar. The Early/Middle Devonian transgression deposited the Muth Formation from Kashmir to Uttarakhand. In Nepal it was somewhat deeper, while it was delayed in Bhutan; therefore deposition commenced in Late Devonian. Elsewhere, sediments grade into siliciclastic-carbonate sequence of the Lipak Formation/Syringothyris Limestone, which range from Givetian to Tournaisian. The latter part is siliciclastic of the Po Formation/Fenestella Shale of Visean Age. There was another uplift during which these sediments contributed clasts to the Late Carboniferous-Early Permian conglomerate (Ganmachidam Formation). In Nepal, the Givetian sediments are disconformably overlain by the Permian. The Early Permian witnessed another transgression (Gechang Formation), which coincided with rifting in Gondwanaland. During the Middle Permian, parts of Kashmir and Zanskar were

sites of volcanicity; elsewhere this was a period of nondeposition. Several lacustrine basins were formed in Kashmir (Nishat Bagh/Mammal Formations) during this volcanism. The Gungri/Zewan Formation represented a more extensive transgression during Wuchiapingian. Except in Kashmir, the Late Changhsingian sediments are absent in other parts with distinct break along the Permian-Triassic interval.

The Triassic sediments (Lilang Supergroup) are mainly shallow marine carbonate-dominated, followed by rapid deepening, which lasted up to Carnian (Chomule Formation/Hedenstromia Beds). Thereafter, the basin gradually shallowed during Middle Norian for extensive coral reef growths, which terminated due to further basin shallowing. There was a minor flooding in lower Upper Norian (Alaror Formation/Monotis Shale) after which Late Norian shallowed to beach environment (Nunuluka Formation/Quartzite Series). The Rhaetic witnessed another flooding and resulted in deposition of overlapped Para Formation/Megalodon limestone. Thereafter, there was a break between the Liassic and Oxfordian (the Upper Callovian break). The Oxfordian to Valanginian Spiti Formation contains ammonoid-bearing black shale throughout the Tethyan sections. In the upper parts, it develops sandstone beds, which pass into the Late Valanginian/Early Hauterivian to Albian Giumal Formation. The sandstone is conformably overlain by limestone and shale of the Chikkim Formation of Campanian/Early Maastrichtian. This part of the Tethyan sequence is absent in Kashmir and Bhutan.

In Zanskar, the ophiolite nappes were emplaced onto the Cretaceous sediments, while deep-facies exotic blocks characterize the Malla Johar Nappe in Uttarakhand. Only in Zanskar, the Thanetian to?Early Ypresian Kelcha Formation is preserved and overlain by paralic to fluvial fining-up arenaceous Dunbar Formation (?Late Ypresian-Lutetian age). There is hiatus between the Cretaceous and Thanetian sediments, as the Danian element is missing.

10.3 Large-Scale Himalayan Tectonics

Since the postulate of collision between India-Asia continents or large-scale underthrusting of India beneath Tibet, various models have been proposed for large-scale tectonics of the Himalaya (Fig. 10.4).

1. *Large-scale underthrusting of India* (Argand 1924): Prior to the advent of plate tectonics, Argand (1924) illustrated underthrusting of India beneath Asia and its 'collision' with the Asian continent beneath Kunlun Mountains and 'not' beneath the Himalaya (Fig. 10.4a). He also documented ductile deformation of the Indian continental crust in south, its doubling up beneath the Himalaya and its rise.
2. *Continent-continent collision* (Dewey and Bird 1970): As a follow-up of plate tectonics and its application to mountain-building processes, Dewey and Bird (1970) formulated concepts of collision-type mountain belts for the Alpine-Himalaya. As India approached and collided with the Asian continent after subduction of its oceanic lithosphere, part of this segment obducted as uppermost ophiolite nappes,

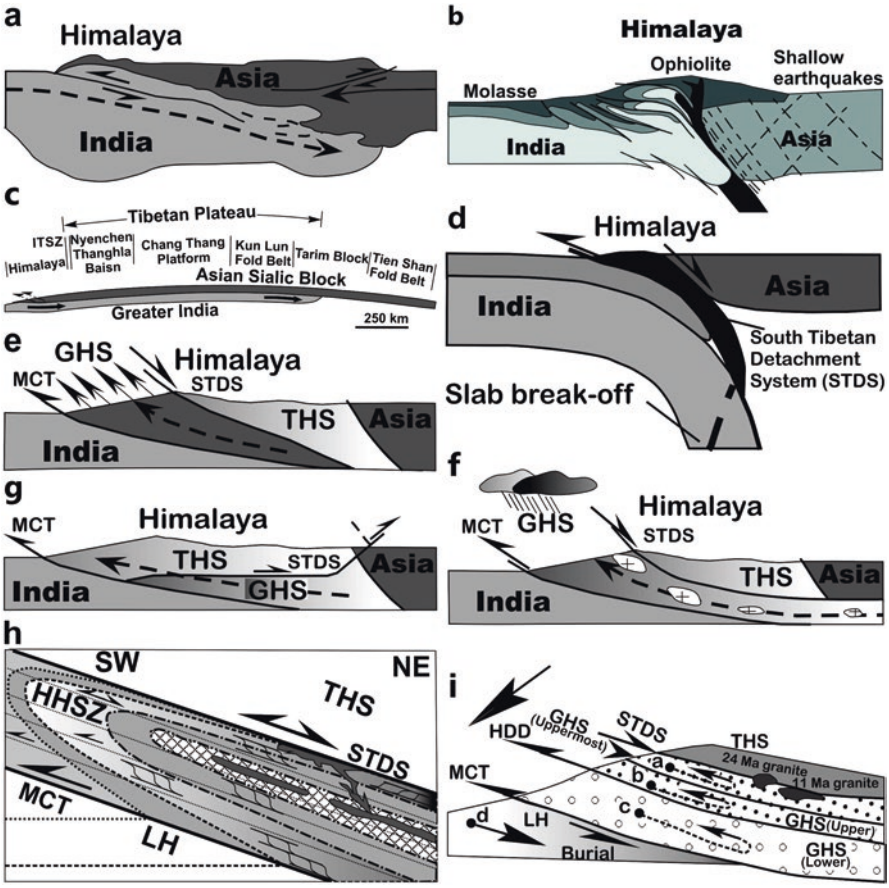

Fig. 10.4 Schematic diagrams showing large-scale tectonic evolution of the Himalaya. (**a**) Large-scale underthrusting of India showing its deformation and extension till Kunlun (Argand 1924). (**b**) Continent-continent collision (Dewey and Bird 1970). (**c**) Underplating of the Indian crust beneath Asia as sub-horizontal slab (Powell and Conaghan 1975). (**d**) Buoyant rise of partially subducted upper continental crustal slice to upper crustal levels, triggered by slab detachment (Chemenda et al. 2000). (**e**) Southward wedge extrusion of high-grade metamorphic complex between non-parallel southward-directed MCT and northward-directed STDS (Burchfiel and Royden 1985). (**f**) Channel flow model of southward migration of partially molten lower and/or middle crustal rocks in a channel and its forced extrusion due to intensified rainfall and resultant erosion (Nelson et al. 1996; Beaumont et al. 2001). (**g**) Tectonic wedging model involving emplacement of the high-grade metamorphic core at depth and bound by thrust-backthrust system (Yin 2006; Webb et al. 2017). (**h**) Intra-continental ductile shear zone model involving high-grade GHS sequence with distributed small-scale S-C penetrative ductile shear zones, causing inversion of metamorphic isograds (shown by thick lines), partial melting and leucogranite generation (Jain and Manickavasagam 1993; Jain et al. 2005). (**i**) In-sequence ductile shearing model involving GHS sequence with downward shifting shearing with time and development of Himalayan discontinuities (Carosi et al. 2018)

which rode southwards over the deformed metamorphosed Indian continent and its platform sediments (Fig. 10.4b). Buoyancy caused the uplift of the Himalaya, its extensive erosion and deposition of molassic sediments into the frontal HFB.

Numerous other tectonic models for evolution of the Himalaya have since been postulated and summarized in Powell and Conaghan (1975) (e.g. Tapponier et al. 1982; Hodges 2000; Yin 2006):

(a) Intra-crustal shortening and thickening by symmetrically divergent penetrative deformation along the India-Asia margins.
(b) Intra-crustal shortening within hot and ductile Asia during convergence of cold India leading to basement reactivation of the Tibetan Plateau.
(c) Repeated southward collision and thrusting of small microcontinental blocks/plates within leading Asian edge throughout Phanerozoic.
(d) India and Tibet belonging to single Gondwanaland fragment with northern edge of the Indian Plate lying beyond the Tibetan Plateau in Tien Shan and the Himalaya evolving intra-continentally.
(e) Indentation/extrusion tectonics by northward rigid India indenter push into softer plastic Asian mass, which caused a narrow Himalayan thrust belt, large-scale strike-slip faulting in Asia and rift zones.

3. *Intra-crustal shortening of Indian subcontinent by underthrusting* (Powell and Conaghan 1973, 1975): Geological settings of various Himalayan and Trans-Himalayan tectonic units made Powell and Conaghan (1973, 1975) to visualize that the Himalaya was produced by large-scale underthrusting of the Gondwanian Indian continent beneath Asia along sub-horizontal crustal fracture with its suturing with Asia along the ITSZ and not directly by continent-continent collision (Fig. 10.4c).
4. *Subducting Indian continental crust* (Chemenda et al. 2000): This model visualized the buoyant rise of detached subducted continental crustal slice to upper levels by compression and buoyancy along the STDS, possibly due to slab detachment at depth (Fig. 10.4d). This slice may be internally soft low viscosity material, flowing in a channel.
5. *Himalayan wedge extrusion model* (Burchfiel and Royden 1985): The MCT and non-parallel north-dipping normal fault system caused southward extrusion of high-grade Himalayan metamorphic tapered core (Fig. 10.4e). Gravitational collapse of overthickened continental crust was proposed as a mechanism for development of the STDS and synchronous movements along the MCT.
6. *Channel flow model* (Nelson et al. 1996): Southward extrusion of high-grade metamorphic rocks and granitic intrusions within the GHS were caused within a low viscosity mid-crustal channel, bounded by the MCT and STDS (also, Beaumont et al. 2001; Godin et al. 2006). A pressure gradient between Tibet and India caused such movements, enhanced by focussed precipitation, erosion and exhumation along southern margin of the Great Himalaya (Fig. 10.4f).
7. *Tectonic wedge model* (Webb et al. 2007): In Himachal, the THS is juxtaposed against the LH sequence along the MCT due to its termination against the STDS. Therefore, the GHS core remains at depth and subsequently forces itself towards the surface (Fig. 10.4g).

8. *Ductile shear model* (Jain and Manickavasagam 1993; Jain et al. 2005): An inverted metamorphism at structurally higher levels across the GHS was explained either by recumbent folding of isograds, structural juxtaposition/thrusting, downward heat transfer from hot plutons/metamorphic belt, shear frictional heating along the MCT or transposition of isograds by simple/general shear. Jain and Manickavasagam (1993) and Jain et al. (2005) proposed that northward subduction of the ICL caused prograde regional metamorphism up to a maximum depth of 25–35 km, when it attained P-T conditions of 5–9 kb and 550–780 °C. Millimetre-spaced C-foliation sigmoidally bent and transposed S-foliation on small-scale towards southwest within a ~20-km-thick non-coaxial intra-continental ductile shear zone (Jain and Manickavasagam 1993). This model postulated that metamorphic isograd surfaces also underwent small-scale displacements by C-foliation with a cumulative displacement of around 80–120 km. Migmatite and leucogranite were produced during decompressional partial melting in sillimanite-muscovite and sillimanite-K-feldspar isograds in upper parts (Fig. 10.4h).
9. *Southward-propagating 'in-sequence' ductile thrusting* (Carosi et al. 2018): The GHS was exhumed during ~25 to 17 Ma by contemporaneous shearing along the MCT and the STDS. Carosi et al. (2018) identified three tectono-metamorphic discontinuities/ductile shear zones since ~40 Ma, with top-to-the-S/SW sense of shear. These progressively exhumed the GHS from uppermost to the lowermost parts, with intervening Higher Himalayan Discontinuity (HHD) (Fig. 10.4i). In-sequence shear model brought more metamorphosed tectonic slices from deeper parts to uppermost structural levels; lowermost unit was juxtaposed at 17–13 Ma along the MCT.

10.4 Exhumation Patterns

The Himalayan orogen experienced variable exhumation, caused either by tectonics or coupled monsoon-controlled erosion (Jain et al. 2000, 2009; Thiede et al. 2009; Patel et al. 2009; Thiede and Ehlers 2013; Clift 2017; Stübner et al. 2018). 'What actually controls exhumation in the Himalayan and adjoining regions' is seriously debated after the postulates of focussed monsoon during the Miocene. In this section, exhumation of monsoon-affected NW Himalaya is compared with monsoon-deficient adjoining regions of the LB and the TMC.

10.4.1 Higher Himalayan Crystallines (HHC)

In the NW Himalaya, the HHC and underlying LH sequences experienced differential exhumation rates during Miocene-Quaternary and are modelled in tectonic framework of fast exhuming windows, thrusts and extensional faults, coupled with rapid erosion (Fig. 10.5a; Jain et al. 2000; Thiede et al. 2009; Patel et al. 2009).

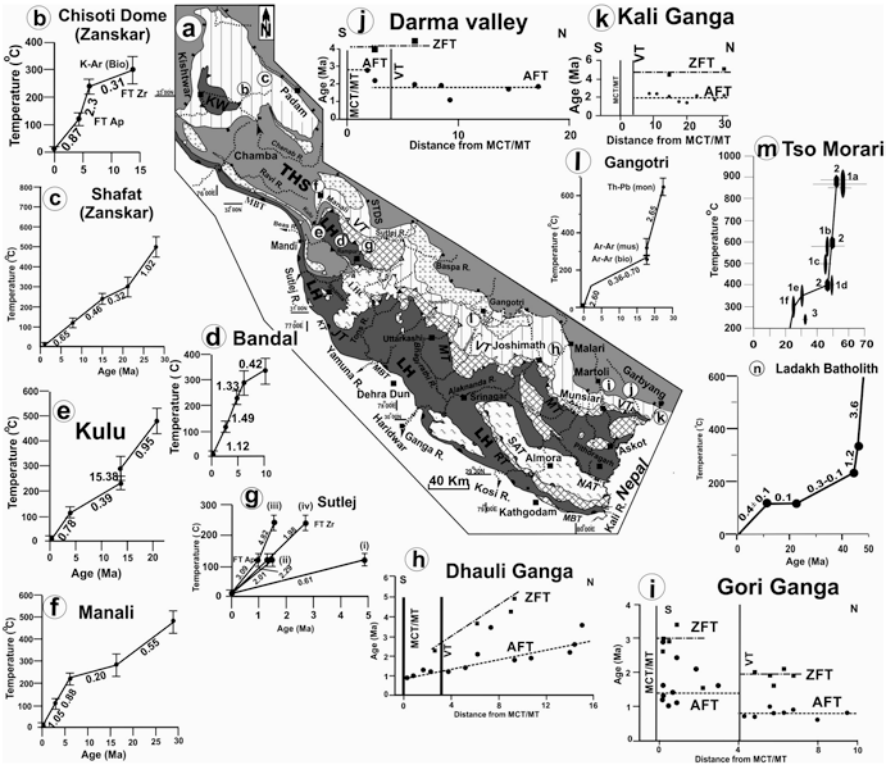

Fig. 10.5 Exhumation paths from the Himalayan Metamorphic Belt (HMB), NW Himalaya, (**a**) Simplified geological map NW Himalaya showing locations of exhumation studies. Refer Fig. 10.2 for details. (**b**–**m**) *T*–*t* curves from Chisoti dome Zanskar (**b**), Shafat and Zanskar (**c**), Bandal (**d**), Kulu (**e**), Manali (**f**), Sutlej Valley (**g**), Dhauli Ganga Valley (**h**), Gori Ganga Valley (**i**), Darma Valley (**j**), Kali Valley (**k**), Gangotri, Bhagirathi Valley (**l**) and Tso Morari (**m**). (Curves redrawn after Jain et al. 2000, 2009, de Sigoyer et al. 2000, Schlup et al. 2003, Leech et al. 2005, 2007, Patel and Carter 2009, Patel et al. 2009)

10.4.1.1 Domes/Windows

Western Himalayan syntaxis witnessed rapid exhumation due to northerly plunging dome and superposed faulting, which caused decrease in $^{40}Ar/^{39}Ar$ biotite ages from ~8.0 to 0.9 ± 0.1 Ma in south central core. The ZFT-AFT ages indicated an enhanced exhumation rate of 5 mm/year during 2.0–0.5 Ma and its further acceleration to 9 mm/year since 0.5 Ma (Winslow et al. 1996).

Suru/Chisoti Domes and Kishtwar/Kulu-Rampur Windows have very young and fast exhumation rates in Jammu and Kashmir: 0.80 mm/year, 1.4 mm/year and 2.97 mm/year, respectively, during 5–l Ma (Kumar et al. 1995; Sorkhabi et al. 1997). In the Chisoti Dome, exhumation rates accelerated from 0.31 mm/year to 2.03 mm/year during 13.7–6.2 Ma and to 4.4 Ma, respectively. Subsequently, it slowed to 0.87 mm/year (Fig. 10.5b). Away from the Suru Dome, exhumation rates ranged from 0.32 to 0.65 mm/year since ~20 Ma (Fig. 10.5c). The Kishtwar window indicated Quaternary folding around 1.0 Ma from its AFT age.

Kulu-Rampur Window exhumed relatively faster than its metamorphic cover along the Beas-Sutlej Valleys. Within the window, the Bandal granite exhibited Late Miocene-Pliocene accelerated exhumation from 0.42 to 1.33 mm/year, as deciphered from $^{40}Ar/^{39}Ar$ sericite, Rb-Sr biotite and ZFT ages (Fig. 10.5d) (see Jain et al. 2000). The ZFT-AFT ages indicated that it finally exhumed at 1.49 ± 0.09 mm/year during 4.50 and 2.68 Ma before slightly slowing down to 1.12 ± 0.18 mm/year. On the southwestern flank of this window around Kulu, exhumation is much faster to 15.38 mm/year for a very short span around 13.7 Ma (Fig. 10.5e) and then much slower (0.55 mm/year) along the northwestern closure during 28.2 and 16.10 Ma (Fig. 10.5f). The Pliocene-Pleistocene accelerated exhumation rates between 1.49 and 1.12 mm/year, measured from the ZFT-AFT and AFT-surface, respectively, surpass all rates within the window zone on limbs and along strike towards northwest (Fig. 10.5e, f). These range from 0.39 to 0.78 mm/year on southwestern flank around Kulu (Fig. 10.5e), between 0.88 and 1.05 mm/year towards northwest between Manali and Rohtang Pass (Fig. 10.5f) and much slower exhumation (0.61 ± 0.10 mm/year) on its northeastern limb since 4.9 Ma (Fig. 10.5g-curve i). All these rates reveal that the MCT has distinctly been active as an extensional normal fault after nappe emplacement on both flanks of the window and facilitated faster exhumation.

10.4.1.2 Thrusts

In the NW Himalaya, the FT ages vary across thrust boundaries, where these have controlled exhumation rates within the HHC in Sutlej Valley and Kumaon, e.g. the Chaura Thrust and the MCT. Along the former, footwall and hanging wall were differentially exhumed at 0.61 ± 0.10 mm/year from 4.9 ± 0.2 to 1.49 ± 0.07 Ma and 2.01 ± 0.35 mm/year from 1.49 ± 0.07 Ma to present (Fig. 10.5g-curves i, ii). However, exhumation rate is 3.09 ± 0.71 mm/year since 0.97 Ma on its hanging wall. The character of the Vaikrita Thrust is uncertain within error limits of average AFT ages of 1.49 ± 0.07 Ma and 1.31 ± 0.22 Ma on both the walls, respectively. The ZFT-AFT ages from the Sutlej Valley reveal interplay of differentially moving crustal wedges both ways during Plio-Pleistocene (Jain et al. 2000).

Along the Dhauli Ganga and Gori Ganga Rivers in eastern Garhwal-Kumaon regions, the AFT ages systematically vary from 0.9 ± 0.3 to 3.6 ± 0.5 Ma from the MT to the north of VT (MCT) in Dhauli Ganga (Fig. 10.5h) in contrast to their stepwise variation across this thrust in the Gori Ganga from 1.6 ± 0.1 to 0.7 ± 0.04 Ma in the hanging wall (Fig. 10.5i). The ZFT ages of 1.8 ± 0.4 Ma remain constant in both the walls (Patel and Carter 2009). Further east along the Darma and Kali Ganga valleys, separated by ~40 km, respective AFT data sets of 1.0 ± 0.1 to 2.8 ± 0.3 Ma and 1.4 ± 0.2 to 2.4 ± 0.3 Ma show very similar exhumation patterns like the Gori Ganga and are controlled by Plio-Quaternary tectonic activity along the Vaikrita Thrust (VT-MCT) (Fig. 10.5j, k; Patel et al. 2009).

Though these valleys possess similar monsoonal conditions, spatio-temporal variations in the ZFT and AFT ages across the MCT zone and the HHC highlight role of thrusts during Pliocene-Pleistocene.

10.4.1.3 Extensional Fault and Erosion

An early Miocene rapid exhumation pulse around 18 Ma is recorded from the Gangotri leucogranite, by $^{40}Ar/^{39}Ar$ muscovite-biotite and ZFT-AFT ages due to the STDS (Fig. 10.5l). Together with Th-Pb monazite ~22.5 Ma age, it appears to have exhumed at a rate of 2.65 mm/year between 23.0 and 18.0 Ma before slowing down to 0.36 and 0.70 mm/year (ZFT-AFT). Another accelerated Late Pliocene-Quaternary exhumation followed at 2.60 mm/year since 1.67 Ma due to rapid erosion (Fig. 10.5l; Jain et al. 2009)

10.4.2 Tso Morari Crystalline (TMC) Belt

After attaining the UHP metamorphism around 53.3 ± 0.7 Ma due to its deep subduction (Leech et al. 2005, 2007), the ICL underwent a record exhumation till ~48–45 Ma from ~120 to 35 km through HP and amphibolite facies (Fig. 10.5m; de Sigoyer et al. 2000). Greenschist facies minerals grew at ~8 km between 45 ± 2 and 34 ± 2 Ma. Thus, the TMC witnessed record maximum exhumation rate of 17 mm/year during ~53 and 50 Ma and subsequent deceleration to 12 mm/year from 50 to 47 Ma, 0.3 mm/year till 34 ± 2 Ma (ZFT) and further lower rate when it attained ~120 °C at 24 ± 2 Ma (AFT) (Guillot et al. 2008).

10.4.3 Trans-Himalayan Ladakh Batholith (LB)

The Ladakh Batholith lacks monsoon precipitation but witnessed an Early-Middle Eocene very fast exhumation of 3.5 ± 0.9 mm/year between 50–45 and 48–45 Ma from closure temperatures of $^{40}Ar/^{39}Ar$ hornblende and Rb-Sr biotite, respectively, and then to 1.2 ± 0.4 mm/year until 43–42 Ma (ZFT age) (Fig. 10.5n; Kumar et al. 2018). Exhumation rates finally decreased during Oligocene to a minimum of ~0.1 mm/a before a mild Late Miocene-Holocene acceleration.

10.5 Timing of India-Asia Convergence

Paleomagnetic and other evidences indicated that estimated timing of closure of the Neo-Tethys along the ITSZ and the India-Asia impingement/'collision' varied between 65 and 35 Ma (Leech et al. 2005; Bouilhol et al. 2013; Jain 2014; Jain 2017). Paleomagnetic anomalies in the Indian Ocean point a slow-down in northward movement of the Indian Plate around 55 ± 1 Ma due to its impingement (Copley et al. 2010; references therein). Paleolatitude evidences reveal an India-Asia suturing of the Himalayan Tethyan succession with Lhasa terrane at 46 ± 8 Ma, when these terranes started overlapping at 22.8 ± 4.2°N paleolatitude (Dupont-

Nivet et al. 2010). Stratigraphically, maximum age of initiation of India-Asia collision in the ITSZ (Ladakh) was deciphered at 56.5–54.9, and minimum age of 50.5 Ma for the closure of the Tethys from termination of continuous marine sedimentation, respectively (Garzanti and van Haver 1988). In this scenario, the ICL travelled to the ITSZ trench at 58 Ma (Garzanti et al. 1987). Renewed clastic supply within the Zanskar sequence revealed closure of the Tethys at ~56 Ma (Sciunnach and Garzanti 2012), though first arrival of Asian-derived detritus in uppermost Tethyan sediments indicated this convergence at ~50 Ma (Najman et al. 2010). Further east in southern Tibet and elsewhere, two-stage collision events at ~55 Ma and younger Oligocene are indicated between an island arc system with India (Event 1) and India-Asia continental collision (Event 2; Aitchison et al. 2007). Similar scenario has been visualized by van Hinsbergen et al. (2012): 50 Ma collision of microcontinent fragment and continental Asia and 25 Ma hard collision.

This timing can, additionally, be resolved by comparing ages of continental subduction (UHP metamorphics—TMC), with oceanic subduction (Ladakh Batholith (LB)). In the TMC, distinct metamorphic events are decipherable from peak UHP, HP eclogite and amphibolites facies at 53.1 ± 0.7, 50.0 ± 0.6 and 47.5 ± 0.5 Ma, respectively. Across the ITSZ, multiple pulsative crystallization and emplacement within the LB are recorded between ~100 and 41 Ma, with its peak crystallization at 57.9 ± 0.3 Ma (Jain 2014). Thus, it is evident that two contrasting deep crustal processes took place ~58 Ma across the ITSZ, leading to the India-Asia contact (Jain 2014).

10.6 Geological Evolution of the Himalaya

After the Tethyan Oceanic lithospheric subduction in the Trans-Himalaya and closure of the Tethyan Ocean (cf. Jain 2014, 2017), subsequent continental lithospheric subduction caused the convergence of the Indian and Asian Plates through various stages; thus evolution of the Himalayan tectonic units can be visualized as follows.

10.6.1 First Stage of Continental Subduction: Tso Morari Crystallines (TMC)

The Indian continental lithosphere (ICL) touched the ITSZ trench at ~58 Ma coinciding with peak plutonic growth of the LB. First stage of continental lithospheric subduction in the Himalaya is, therefore, recorded along leading edge of the Indian Plate in Tso Morari, where it subducted down to depth of ~120 km to produce carbonate-coesite-bearing UHP eclogite at >39 kb, >750 °C and 53.1 ± 0.7 Ma and subsequent retrogression to HP and amphibolite facies between 50.0 and 48 Ma, respectively (Fig. 10.6; Guillot et al. 1997; Leech et al. 2005, 2007). $^{40}Ar/^{39}Ar$ mica and ZFT ages provide evidences of late-stage exhumation and shallow crustal stabilization between 45.0 and 34.0 2 Ma (Schlup et al. 2003). Thus, the TMC exhumed very fast ca. 1.7 cm/year between 53 and 50 Ma and 1.2 cm/year between 50 and 47 Ma and then slowed down to ca. 0.3 cm/year till 35 Ma (Guillot et al. 2008).

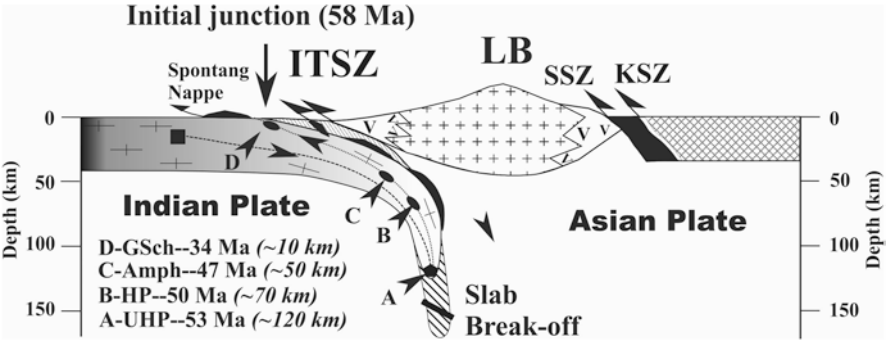

Fig. 10.6 Steep continental lithospheric subduction of the Indian Plate in the TMC, its UHP metamorphism and exhumation. Development of gneiss-hosted UHP eclogite at 53.1 ± 0.7 Ma. The TMC follows same exhumation and cooling paths through various metamorphic facies. See text for details. During the HP facies, steeply subducted continental lithosphere melted along southern margin of the Ladakh Batholith to produce crustal contaminations

The Himalaya first emerged in the Tso Morari region between 53 and 50 Ma when continental crust was exhumed from ~120 km depth. The terrane was uplifted very fast rate to near-surface and eroded off to shed detritus into the HFB in the south and the ITSZ basin (Jain et al. 2009). This subducting lithospheric slab did not melt till its decompression around 50 Ma after the HP metamorphism. Very steep geometry of the Indian lithosphere and its melting along the ITSZ, thus, explains sharp isotopic changes in the overlying LB along its southern margin.

10.6.2 Second Stage of Continental Subduction: HHC

Folded HMB slab underwent peak Late Eocene pre-MCT regional Barrovian metamorphism in upper amphibolite facies at 650–700 °C, 8–9 kb and around 45–35 Ma (Hodges 2000; Foster et al. 2000) (Fig. 10.7). It is likely that the ICL underwent shallow continental subduction along the proto-MCT to a depth of 25–35 km after subduction in Tso Morari region. $^{40}Ar/^{39}Ar$/K-Ar hornblende and muscovite ages gave its cooling through 500 ± 50 °C and 350 ± 50 °C between 40 and 30 Ma (Sorkhabi et al. 1999a, b).

10.6.3 Third Stage of Continental Subduction: Within HHC

Within the HHC belt, younger Miocene ~25 Ma metamorphism and partial melting led to leucogranite generation between 25 and 15 Ma, though leucosome melt production also took place occasionally during the Eocene and Oligocene (33–23 Ma) (Carosi et al. 2018). These melts appear to have evolved in a southward extruding Himalayan orogenic channel, bounded by the MCT and STDS (Grujic 2006).

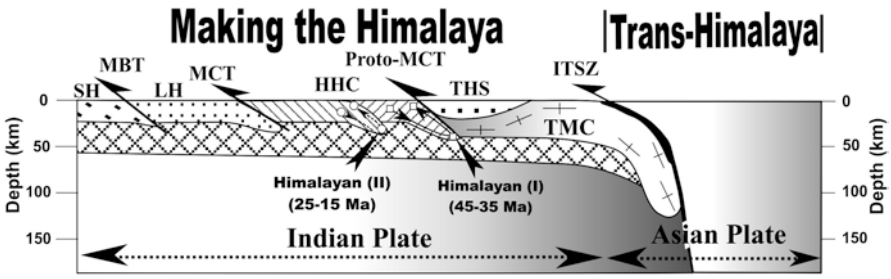

Fig. 10.7 Continental subduction in the NW Himalaya. Shallower and younger continental subduction in the HHC produced peak Eocene (~48–45 Ma) and pre-MCT metamorphism in upper amphibolite facies. Younger Miocene ~25 Ma metamorphism, anataxis and leucogranite generation between 25 and 15 Ma. Major discontinuities within HHC caused its differential exhumation. See Carosi et al. (2018) for details. Thrusting and imbrication along the MBT and MFT during late Miocene-Pliocene-Pleistocene

Subsequent Miocene–Pleistocene exhumation is widespread in the HHC, followed by its extensive erosion to produce detritus for the Cenozoic Himalayan foreland and Indo-Gangetic-Bengal basins (Hodges 2000; Yin 2006); these patterns are either controlled by tectonics, concomitant erosion or a combination of two processes (Jain et al. 2000).

10.7 Present-Day Configuration

During the past two decades, configuration of the Indian Plate beneath the Himalaya and adjoining regions has been imaged by magnetotelluric profiling, seismic tomography and focal plane mechanism of recent earthquakes.

10.7.1 Magnetotelluric (MT) Evidences

Magnetotelluric (MT) profiles from the NW Himalaya image the present-day geometry of the Indian Plate (IP) (Fig. 10.8a). Along Roorkee-Gangotri profile (Uttarakhand), the Precambrian basement (>1000 Ωm electrical resistivity) is overlain by a northerly gently dipping and 7-km-thick veneer of Miocene-Recent conducting sediments (<50 Ωm) within the Indo-Gangetic Plains (IGP) and Sub-Himalaya. Their contacts represent fluid-saturated fractured zone of the Main Himalayan Thrust (MHT) along which the IP subducts beneath the Himalaya (Israil et al. 2008; Miglani et al. 2014). A sharp discontinuity defines the MBT where resistivity increases in the Precambrian LH belt. Below the MHT-controlled conductor, high electrical resistive zone at ~30 km depth represents northerly subducting IP continental crust (Miglani et al. 2014). Fluid-filled fractured MHT zone of very low

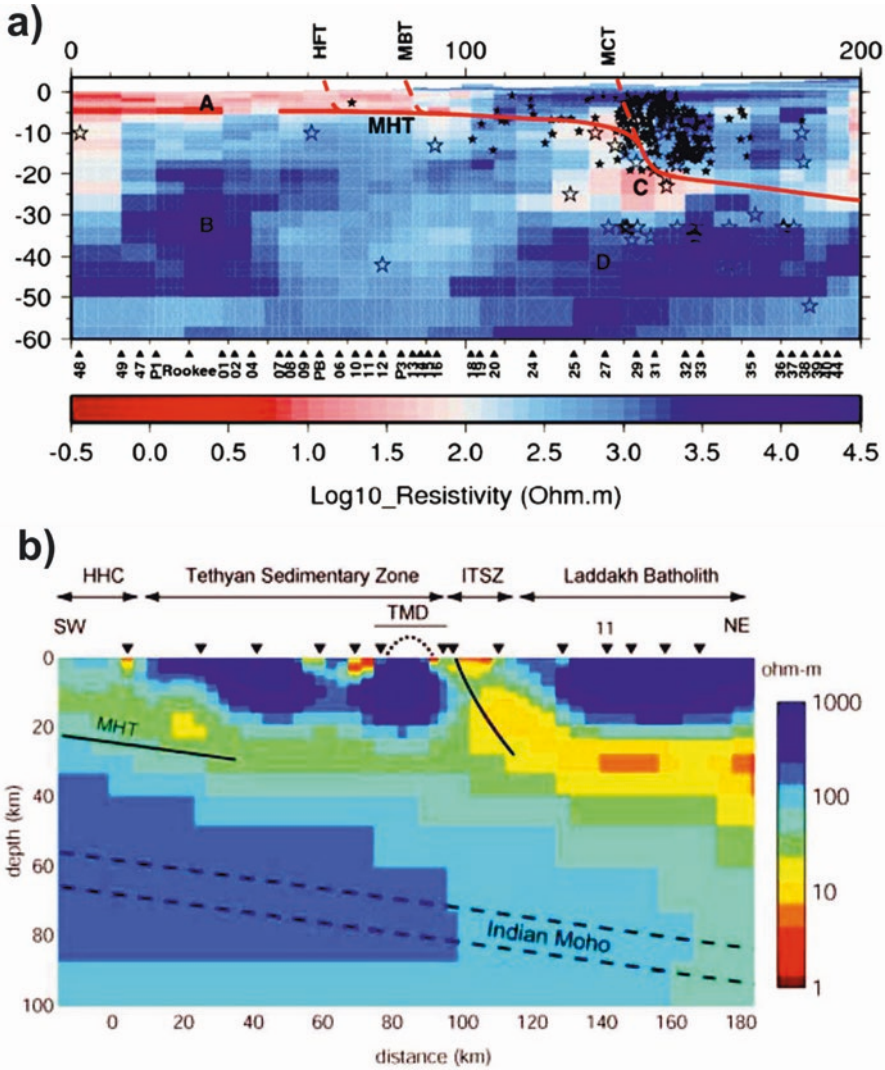

Fig. 10.8 Magnetotelluric sections from the NW Himalaya to Karakoram. (**a**) MT section along Roorkee-Gangotri profile showing low resistivity (<10 Ωm) zone beneath MCT and cluster of small associated earthquakes (Miglani et al. 2014). (**b**) Deep resistivity structure of the subducting Indian lithosphere along Tso Morari and further northeast. NE-dipping low resistivity zone (~30 Ωm-white colour) is observed beneath THS, Tso Morari dome (TMD) and beyond where it becomes sub-horizontal beneath ITSZ and LB (Arora et al. 2007)

<10 Ωm resistivity extends up to a depth of ~30 km within a ramp and is marked by earthquake cluster and heat flow. Further southeast along the Bijnor-Joshimath-Malari traverse (Uttarakhand), ~5-km-thick low-angle and NE-dipping intra-crustal high conducting layer (IC-HCL) of very low resistivity is observed across the IGP

and the Higher Himalaya with an intervening ramp (Rawat et al. 2014); the whole structure also controls velocities of seismic waves in intra-crustal low velocity layer (IC-LVL) (Caldwell et al. 2013). These layers are fluid-saturated due to partial melt or released water from metamorphic reactions.

This mid-crustal conductor of low resistivity zone may also indicate partial melt in extreme northeast between Tso Morari and beyond, where its sub-horizontal geometry extends beneath high resistive LB and Karakoram Batholith (Fig. 10.8b; Gokarn et al. 2002; Arora et al. 2007).

10.7.2 Seismological Evidences

Seismic tomography, reflection profiles, earthquakes and their fault-plane solutions from the Himalayan arc and Tibet provide constraints on the present-day configuration of the Indian Plate. In NW Himalaya, the Moho runs almost parallel below low resistivity layer and defines geometry of the subducting ICL even beyond Karakoram fault (Rai et al. 2006). The majority of earthquakes are located within a narrow belt between north-dipping MBT and the MCT and are essentially controlled by a mid-crustal ramp within the MHT along which the Indian Plate underthrusts southern Tibet at about 10° (Seeber et al. 1981; Ni and Barazangi 1984; Nelson et al. 1996). This surface dips at ~15° from about 10 to 20 km depth within the Himalaya and controls focal mechanisms not only of shallow ($\lesssim$30°) earthquakes but also the great Himalayan earthquakes of $M > 8$ (Ni and Barazangi 1984). Outer seismic mid-crustal ramp extends into an aseismic 30–40-km-deep seismic reflector, imaged in the INDEPTH experiment further north (Zhao et al. 1993).

Subducted Indian lower crust does not stop at the ITSZ/IYS, but it underthrusts and extends northwards beneath the partially molten Asian crust till Bangong-Nujiang Suture (BNS) where both the Indian and Asian lithospheric mantles subduct downwards due to flow (Fig. 10.9; Nábělek et al. 2009; Liang et al. 2012). Recent deep seismic reflection profiles by Guo et al. (2017) across ITSZ further strengthen a crustal-scale outline of the subducting Indian crust.

10.8 Discussions and Conclusions

Geological setting of various Himalayan units clearly demonstrates that leading northernmost ICL was juxtaposed against the Trans-Himalayan ITSZ and LB and not with any tectonic unit of the Asian continental lithosphere. It converged first with the intra-oceanic Shyok-Dras volcanic island arc, which existed within the Tethyan Ocean, and then both of them moved towards the Indian continental margin (Stampfli and Borel 2002; Rolland et al. 2002; Maheo et al. 2004) or vice versa (Bouilhol et al. 2013). It is evident that Indian and Asian continental lithospheres, separated by Neo-Tethys, did not initially ‘collide’ directly to make the Himalaya (cf., Powell and Conaghan 1973).

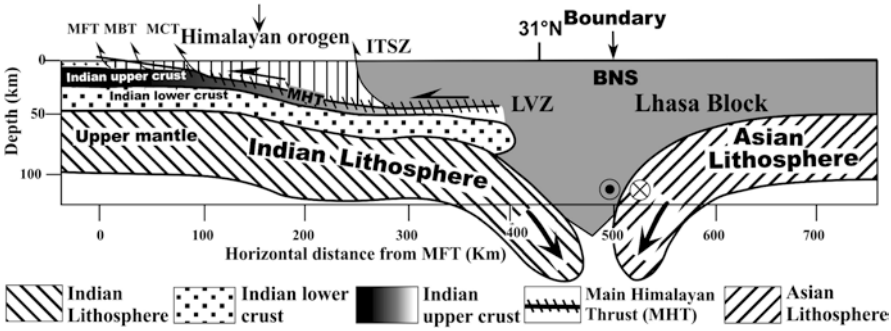

Fig. 10.9 Simplified geophysical cross-section of the India-Asia convergence beneath the Himalaya and Tibet from the Hi-CLIMB profile, depicting 'collision' between two plates in the Bangong-Nujiang Suture (BNS). Large-scale tectonics of the Himalayan orogen is depicted as scrapped crustal wedge above the MHT and its limits by the ITSZ. (Redrawn after Nábělek et al. 2009)

As the Neo-Tethys finally closed along the ITSZ during Paleocene, timing of first India-Asia impingement is constrained at ~58 Ma by comparing ages of the Trans-Himalayan LB with the TMC. Both the LB and the TMC signify drastic geodynamic changes within ~4–5 Ma across the ITSZ.

At the time of India undergoing UHP metamorphism at ~53 Ma in Tso Morari steep subduction zone, the ITSZ limited the Indian continental lithosphere. As the steep ICL took some time to reach depth of about ~120 km to have suffered UHP metamorphism from near surface, difference of ~4–5 Ma in these values is accounted for fast speed by which the plate underwent the subduction. This steep continental lithosphere subduction and its melting along the southern margin can account for younger pulses within the LB with more evolved isotopic signatures till 45 Ma without modifying the proposed age of the India-Asia contact (cf., Bouilhol et al. 2013).

It is likely that the Himalaya first witnessed its rise and emergence during 53 and 50 Ma in the Tso Morari, when part of continental lithosphere exhumed after undergoing UHP metamorphism. Further imbrication and subduction of the ICL caused its two metamorphisms and associated exhumation episodes within the HHC during 45–35 and 25–15 Ma, respectively, for the rise of the Himalayan Mountains (Fig. 10.7). It is clearly implied that original configuration of the ICL must have been very different, steeper and imbricated than the present-day geometry (O'Brien et al. 2001), which is attained by its northerly push and flattening of imbricated Himalayan packages, now lying sub-horizontally (Fig. 10.10).

Present-day geometry of the Indian continental lithosphere beneath the Himalaya and beyond in Asia reflects its unique subducting near-horizontal configuration. Low resistivity zone (5–10 Ωm) of partial melt/fluid-rich mid-crustal layer at 15–25 km above the MHT defines the top of the IP, which is underlain by relatively high electrical resistive ICL. This layer is observed throughout the Himalaya and beyond and is the first-order structure in the northwest. A steeper northeast-dipping low resistivity zone beyond Tso Morari flattens out at depth beneath the LB and merges with this first-order conductor (Arora et al. 2007).

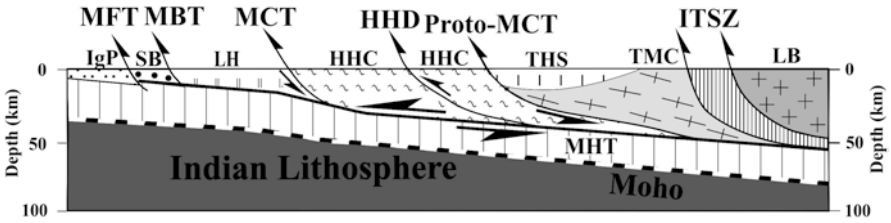

Fig. 10.10 Rotated imbricated slices of the Himalayan Metamorphic Belt (HMB) to gently dipping crustal wedges of the TMC, HHC including its Higher Himalayan Discontinuities (HHD) by northward push of the subducting Indian continental lithosphere along the MHT since post-15 Ma. Configuration is based upon the present-data magnetotelluric data from Garhwal and Ladakh-Karakoram. The MHT approximately follows upper–lower continental crust boundary (vertical lines). Indian lithosphere shown by tiny squares and Moho follows its upper contact

Seismologically, the majority of earthquakes and tomographic evidences delineate a basal MHT within the Indian Plate along which it subducts beneath the southern Tibet at about 10° or less (Nelson et al. 1996). In fact, signatures of the ICL extend northwards beneath the partially molten Asian crust till BNS, where both the Indian and Asian lithosphere mantles subduct northwards and southwards, respectively.

Thus, critical geological and geophysical evidences from the Himalaya and adjoining mountains lead us to postulate that the Indian continental lithosphere (ICL) subducted and imbricated sequentially in geological past since 58 Ma. The overriding sequences were scrapped, thrust southward along the MCT-MBT systems and deformed as crustal wedges in the rising Himalaya whose erosion caused deposition into the frontal Himalayan foreland basin and the Indo-Gangetic Plains because of tectonics and monsoonal precipitation since Miocene. The Indian and Asian Plates interacted and ‘collided’ only in the Bangong-Nujiang Suture (BNS).

Acknowledgements This chapter has emerged from many field expeditions in Karakoram, Ladakh and adjoining regions, which were funded by Department of Science and Technology, New Delhi. Sandeep Singh from the IIT Roorkee has been an inspiration to explore more along with many other students. Thanks are due to Indian National Science Academy, New Delhi, for the awards of Senior and Honorary Scientist Schemes and to Dr. N. Gopikrishnan, Director, CSIR-Central Building Research Institute, Roorkee, for the facilities.

Discussions with V.C. Thakur and P.K. Mukherjee (Dehradun) on tectonics of Ladakh and Md. Israil and V.K. Gahlaut on geophysical aspects were extremely useful in clearing many doubts. O.N. Bhargava has been instrumental in highlighting many shortcomings in this write-up and also contributing to the geology of the Tethys.

Thanks are due to S.K. Tandon and Neal Gupta for the invitation to write this chapter and for providing critical comments on this chapter. The author appreciates gesture of Md Israil and B.R. Arora for providing me the original drawings of Fig. 10.10.

References

Aitchison JC, Ali JR, Davis AM (2007) When and where did India and Asia collide? J Geophys Res 112:B05423. https://doi.org/10.1029/2006JB004706

Argand E (1924) La tectoniquedel’ Asie. Proc 13th Int Geol Cong 7:170–372

Arora BR, Unsworth MJ, Rawat G (2007) Deep resistivity structure of the northwest Indian Himalaya and its tectonic implications. Geophys Res Lett 34:L04307. https://doi.org/10.1029/2006GL029165

Beaumont C, Jamieson RA, Nguyen MH, Lee B (2001) Himalayan tectonics explained by extrusion of a low-viscosity crustal channel coupled to focused surface denudation. Nature 414:738–742. https://doi.org/10.1038/414738a

Bhargava ON (2008) An updated introduction to the Spiti geology. J Palaeont Soc India 53(2):93–129

Bhargava ON, Srikantia SV (2014) Geology and age of metamorphism of the Jutogh and Vaikrita Thrust Sheets, Himachal Himalaya. Himalayan Geol 35(1):1–15

Bhatia SB, Bhargava ON (2006) Biochronological continuity of the Paleocene sediments of the Himalayan Foreland Basin: paleontological and other evidences. J Asian Earth Sci 26:477–487

Bouilhol P, Jagoutz O, Hanchar JM, Dudas FO (2013) Dating the India-Eurasia collision through arc magmatic records. Earth Planet Sci Lett 366:163–175

Burchfiel BC, Royden LH (1985) North-south extension within the convergent Himalayan region. Geology 13:679–682

Caldwell WB, Klemperer SL, Lawrence JF, Rai SS, Ashish (2013) Characterizing the Main Himalayan Thrust in the Garhwal Himalaya, India with receiver function CCP stacking. Earth Planet Sci Lett 367:15–27

Carosi R, Montomoli C, Iaccarino S (2018) 20 years of geological mapping of the metamorphic core across Central and Eastern Himalayas. Earth-Sci Rev 177:124–138

Chemenda AI, Burg JP, Mattauer M (2000) Evolutionary model of the Himalaya–Tibet system: geopoem based on new modeling, geological and geophysical data. Earth Planet Sci Lett 174:397–409

Clift PD (2017) Cenozoic sedimentary records of climate-tectonic coupling in the Western Himalaya. Prog Earth Planet Sci 4:39. https://doi.org/10.1186/s40645-017-0151-8

Copley A, Avouac JP, Royer JY (2010) India-Asia collision and the Cenozoic slowdown of the Indian plate: implications for the forces driving plate motions. J Geophys Res 95:B03410. https://doi.org/10.1029/2009JB006634

de Sigoyer J, Chavagnac V, Blichert-Toft J, Villa IM, Luais B, Guillot S, Cosca M, Mascle G (2000) Dating the Indian continental subduction and collisional thickening in the northwest Himalaya: multichronology of the Tso Morari eclogites. Geology 28:487–490

Dewey JF, Bird JM (1970) Mountain belts and the new global tectonics. J Geophys Res 75:2625–2647

Dupont-Nivet G, van Hinsbergen DJJ, Torsvik TH (2010) Persistently low Asian paleolatitudes: implications for the India-Asia collision history. Tectonics 29:TC5016. https://doi.org/10.1029/2008TC002437

Foster G, Kinny P, Vance D, Prince C, Harris N (2000) The significance of monazite U-Th-Pb age data in metamorphic assemblage; a combined study of monazite and garnet chronometry. Earth Planet Sci Lett 181:327–340

Garzanti E, van Haver T (1988) The Indus clastics: forearc basin sedimentation in the Ladakh Himalaya (India). Sediment Geol 59:237–249

Garzanti E, Baud A, Mascle G (1987) Sedimentary record of the northward flight of India and its collision with Eurasia (Ladakh Himalaya, India). Geodynam Acta 1:297–312

Godin L, Grujic D, Law RD, Searle MP (2006) Channel flow, ductile extrusion and exhumation in continental collision zones: an introduction. In: Law RD, Searle MP, Godin L (eds) Channel flow, ductile extrusion and exhumation in continental collision zones, Geol Soc Spec Publ, vol 268. Geological Society, London, pp 1–23

Gokarn SG, Gupta G, Rao CK, Selvaraj CB (2002) Electrical structure across the Indus Tsangpo suture and Shyok suture zones in NW Himalaya using magnetotelluric studies. Geophys Res Lett 29(8):1251. https://doi.org/10.1029/2001GL014325

Grujic D (2006) Channel flow and continental collision tectonics. In: Law RD, Searle MP, Godin L (eds) Channel flow, ductile extrusion and exhumation in continental collision zones, Geol Soc Spec Publ, vol 268. Geological Society, London, pp 25–37

Guillot S, de Sigoyer J, Lardeaux JM, Mascle G (1997) Eclogitic metasediments from the Tso Morari area (Ladakh, Himalaya): evidence for continental subduction during India-Asia convergence. Contrib Mineral Petrol 128:197–212

Guillot S, Mahéo G, de Sigoyer J, Hattori KH, Pêcher A (2008) Tethyan and Indian subduction viewed from the Himalayan high-to ultrahigh-pressure metamorphic rocks. Tectonophysics 451:225–241

Guo X, Li W, Gao R, Xu X, Li H, Huang X, Ye Z, Lu Z, Klemper SL (2017) Nonuniform subduction of the Indian crust beneath the Himalayas. Sci Rep 7:12497. https://doi.org/10.1038/s41598-017-12908-0

Heim A, Gansser A (1939) Central Himalaya: geological observations of the Swiss expedition, Mem de la Société Helvetique des Sci Naturelles, vol 73. Gebrüder Fretz, Zürich. 245p

Hodges KV (2000) Tectonics of the Himalaya and southern Tibet from two perspectives. Geol Soc Am Bull 92:324–350

Hofmann M, Linnemann U, Rai V, Becker S, Gärtner A, Sagawe A (2011) The India and South China cratons at the margin of Rodinia—Synchronous Neoproterozoic magmatism revealed by LA-ICP-MS zircon analyses. Lithos 123:176–187

Honegger K, Dietrich V, Frank W, Gansser A, Thoni M, Trommsdorff V (1982) Magmatism and metamorphism in the Ladakh Himalaya the Indus-Tsangpo suture zone. Earth Planet Sci Lett 60:253–292

Israil M, Tyagi DK, Gupta PK, Niwas S (2008) Magnetotelluric investigations for imaging electrical structure of Garhwal Himalayan corridor, Uttarakhand, India. J Earth Syst Sci 97:189–200

Jain AK (2014) When did India-Asia collide and make the Himalaya? Curr Sci 106(2):254–266

Jain AK, Manickavasagam RM (1993) Inverted metamorphism in the intra-continental ductile shear zone during Himalayan collision tectonics. Geology 21:407–410

Jain AK, Singh S (2008) Tectonics of the southern Asian Plate margin along the Karakoram Shear Zone: constraints from field observations and U-Pb SHRIMP ages. Tectonophysics 451(1–4):186–205

Jain AK, Singh S (2009) Geology and tectonics of the southeastern Ladakh and Karakoram. Geological Society of India, Bangalore, India. 179p

Jain AK, Kumar D, Singh S, Kumar A, Lal N (2000) Timing, quantification and tectonic modeling of Pliocene Quaternary movements in the NW Himalaya: evidences from fission track dating. Earth Planet Sci Lett 179:437–451

Jain AK, Singh S, Manickavasagam RM (2002) Himalayan collision tectonics. Gondwana Res Group Mem 7:94

Jain AK, Singh S, Manickavasagam RM, Joshi M, Verma PK (2003) HIMPROBE Programme: integrated studies on geology, petrology, geochronology and geophysics of the Trans-Himalaya and Karakoram. Mem Geol Soc India 53:1–56

Jain AK, Manickavasagam RM, Singh S, Mukherjee S (2005) Himalayan collision zone: new perspectives - its tectonic evolution in a combined ductile shear zone and channel flow model. Himal Geol 26(1):1–18

Jain AK, Lal N, Sulemani B, Awasthi AK, Singh S, Kumar R, Kumar D (2009) Detrital-zircon fission track geochronology of the Lower Cenozoic sediments, NW Himalayan foreland basin: clues for exhumation and denudation of the Himalaya during India-Asia collision. Geol Soc Am Bull 121:519–535

Jain AK (2017) Continental subduction in the NW-Himalaya and Trans-Himalaya. Ital J Geosci 136 (1):89–102, https://doi.org/10.3301/IJG.2015.43

Jain AK, Shrestha M, Seth P, Kanyal L, Carosi R, Montomoli C, Iaccarino S, Mukherjee PK (2014) The Higher Himalayan Crystallines, Alaknanda–Dhauli Ganga Valleys, Garhwal Himalaya, India. In: Montomoli C, Carosi R, Law RD, Singh S, Rai SM (eds) Geological field trips in the Himalaya, Karakoram and Tibet. J Virtual Expl, Electr Edit 47 paper 8, ISSN 1441–8142

Kohn MJ (2014) Himalayan metamorphism and its tectonic implications. Annu Rev Earth Planet Sci 42:381–419

Kumar A, Lal N, Jain AK, Sorkhabi RB (1995) Late Cenozoic-Quaternary thermotectonic history of Higher Himalayan Crystallines (HHC) in Kishtwar-Padar-Zanskar region, NW Himalaya: evidence from fission track ages. J Geol Soc India 45:375–391

Kumar R, Ghosh SK, Sangode SJ (2009) Sedimentary architecture of Late Cenozoic Himalayan Foreland Basin fill: an overview. Mem Geol Soc India 78:245–280

Kumar R, Jain AK, Lal N, Singh S (2018) Early-Middle Eocene exhumation of the Trans-Himalayan Ladakh Batholith, and the India-Asia convergence. Curr Sci 113:1090–1098
Leech ML, Singh S, Jain AK, Klemperer SL, Manickavasagam RM (2005) Early, steep subduction of India beneath Asia required by early UHP metamorphism. Earth Planet Sci Lett 234:83–97
Leech ML, Singh S, Jain AK (2007) Continuous metamorphic zircon growth and interpretation of U-Pb SHRIMP dating: an example from the Western Himalaya. Int Geol Rev 49:313–328
Liang X, Sandvola E, Chen YJ, Hearn T, Ni J, Klemperer S, Shen Y, Tilmann F (2012) A complex Tibetan upper mantle: a fragmented Indian slab and no south-verging subduction of Eurasian lithosphere. Earth Planet Sci Lett 333–334:101–191
Maheo G, Bertrand H, Guillot S, Villa IM, Keller F, Capiez P (2004) The south Ladakh ophiolites (NW Himalaya, India): an intra-oceanic tholeiitic origin with implication for the closure of the Neo-Tethys. Chem Geol 203:273–303
Mandal S, Robinson DM, Khanal S, Das O (2015) Redefining the tectonostratigraphic and structural architecture of the Almora klippe and the Ramgarh-Munsiari Thrust sheet in NW India. In: Mukherjee S, Carosi R, van der Beek PA, Mukherjee BK, Robinson DM (eds) Tectonics of the Himalaya, Geol Soc London Spec Publ, vol 412. Geological Society, London, pp 247–269
Mandal S, Robinson DM, Kohn MJ, Khanal S, Das O, Bose S (2016) Zircon U-Pb ages and Hf isotopes of the Askot klippe, Kumaun, northwest India: implications for Paleoproterozoic tectonics, basin evolution and associated metallogeny of the northern Indian cratonic margin. Tectonics 35:965–982. https://doi.org/10.1002/2015TC004064
Miglani R, Shahrukh M, Israil M, Gupta PK, Varsheney SK, Sokolova E (2014) Geoelectric structure estimated from magnetotelluric data from Uttarakhand Himalaya, India. J Earth Syst Sci 123(8):907–918
Myrow PM, Hughes NC, Paulsen TS, Williams IS, Parcha SK, Thompson KR, Bowring SA, Peng S-C, Ahluwalia AD (2003) Integrated tectonostratigraphic reconstruction of the Himalaya and implications for its tectonic reconstruction. Earth Planet Sci Lett 212:433–441
Nábělek J, Hetenyi G, Vergne J, Sapkota S, Kafle B, Jiang M, Su H, Chen J, Huang B-S, The HI-CLIMB Team (2009) Underplating in the Himalaya-Tibet collision zone revealed by the Hi-CLIMB experiment. Science 325:1371–1374
Najman Y (2006) The detrital record of orogenesis: a review of approaches and techniques used in the Himalayan sedimentary basins. Earth-Sci Rev 74(1–2):1–72
Najman Y, Bickle M, Chapman H (2000) Early Himalayan exhumation: isotopic constraints from the Indian foreland basin. Terra Nova 12:28–34
Najman Y, Appel E, Boudagher-Fadel M, Bown P, Carter A, Garzanti E, Godin L, Han JT, Liebke U, Oliver G, Parrish R, Vezzoli G (2010) Timing of India-Asia collision: geological, biostratigraphic, and palaeomagnetic constraints. J Geophys Res 95:B12416
Nelson KD, Zhao W, Brown LD, Indepth Team (1996) Partially molten middle crust beneath southern Tibet: synthesis of Project INDEPTH results. Science 274:1684–1688
Ni JF, Barazangi M (1984) Seismotectonics of the Himalayan collision zone: geometry of the underthrusting Indian plate beneath the Himalaya. J Geophys Res 89:947–963
O'Brien PJ, Zotov N, Law R, Khan MA, Jan MQ (2001) Coesite in Himalayan eclogite and implications for models of India-Asia collision. Geology 29(5):435–438
Patel RC, Carter A (2009) Exhumation history of the Higher Himalayan Crystalline along Dhauliganga-Goriganga river valleys, NW India: new constraints from fission-track analysis. Tectonics 28:TC3004. https://doi.org/10.1029/2008TC002373
Patel RC, Adlakha V, Lal N, Singh P, Kumar Y (2009) Spatiotemporal variation in exhumation of the Crystallines in the NW-Himalaya, India: constraints from Fission Track dating analysis. Tectonophysics 504(1–4):1–13
Powell CMA, Conaghan PJ (1973) Plate tectonics and the Himalayas. Earth Planet Sci Lett 20(1):1–12. https://doi.org/10.1016/0012-821X(73)90134-9
Powell CMA, Conaghan PJ (1975) Tectonic models of the Tibetan plateau. Geology 3:727–731. https://doi.org/10.1130/0091-7613(1975)3<727:TMOTTP>2.0.CO;2
Rahaman W, Singh SK, Sinha R, Tandon SK (2009) Climate control on erosion distribution over the Himalaya during the past ~100 ka. Geology 37(6):559–562. https://doi.org/10.1130/G25425A.1

Rai SS, Priestley K, Gaur VK, Mitra S, Singh MP, Searle MP (2006) Configuration of the Indian Moho beneath the NW Himalaya. Geophys Res Lett 33:L15308. https://doi.org/10.1029/2006GL026076

Rawat G, Arora BR, Gupta PK (2014) Electrical resistivity cross-section across the Garhwal Himalaya: proxy to fluid-seismicity linkage. Tectonophysics 637:68–79

Rolland Y, Pêcher A, Picard C (2000) Middle Cretaceous back-arc formation and arc evolution along the Asian margin: the Shyok Suture Zone in northern Ladakh NW Himalaya. Tectonophysics 325:145–173

Rolland Y, Picard C, Pêcher A, Lapierre H, Bosch D, Keller F (2002) The cretaceous Ladakh arc of NW Himalaya—slab melting and melt-mantle interaction during fast northward drift of Indian Plate. Chem Geol 182:139–178

Schlup M, Carter A, Cosca M, Steck A (2003) Exhumation history of eastern Ladakh revealed by $^{40}Ar/^{39}Ar$ and fission track ages: the Indus river-Tso Morari transect, NW Himalaya. J Geol Soc Lond 160:385–399

Sciunnach D, Garzanti E (2012) Subsidence history of the Tethys Himalaya. Earth-Sci Rev 111:179–198

Searle MP, Windley BF, Coward MP, Cooper DJW, Rex AJ, Rex D, Tingdong L, Xuchang X, Jan MQ, Thakur VC, Kumar S (1987) The closing of the Tethys and the tectonics of the Himalaya. Geol Soc Am Bull 98:678–701

Seeber L, Armbruster JG, Quittmeyer R (1981) Seismicity and continental subduction in the Himalayan Arc. In: Gupta HK, Delany FM (eds) Zagros, Hindu Kush, Himalaya geodynamic evolution, Geodynamic Series, vol 4. American Geophysical Union, Washington, DC, pp 215–242

Singh IB (1999) Tectonic control on sedimentation in Ganga Plain Foreland Basin: constraints on the Siwalik sedimentation models. In: Jain AK, Manickavasagam RM (eds) Geodynamics of the NW Himalaya, Gondwana Res Group Mem, vol 6. Gondwana Research Group, Gondwana, pp 3–37

Sorkhabi RB, Jain AK, Itaya T, Fukui S, Lal N, Kumar A (1997) Cooling age record of domal uplift in the core of the Higher Himalayan Crystallines (HHC) southwest Zanskar, India. Proc Indian Acad Sci Earth Planet Sci 106:169–179

Sorkhabi RB, Stump E, Foland K, Jain AK (1999a) Tectonics and cooling history of the Garhwal Higher Himalaya (Bhagirathi Valley): constraints from thermochronological data. In: Jain AK, Manickavasagam RM (eds) Geodynamics of the NW Himalaya, Gondwana Res Group Mem, vol 6. Gondwana Research Group, Gondwana, pp 217–235

Sorkhabi RB, Valdiya KS, Arita K (1999b) Cenozoic uplift of the Himalayan Orogen: chronologic and kinematic patterns. In: Jain AK, Manickavasagam RM (eds) Geodynamics of the NW Himalaya, Gondwana Res Group Mem, vol 6. Gondwana Research Group, Gondwana, pp 189–206

Srikantia SV, Bhargava ON (1998) Geology of Himachal Pradesh, Mem Geol Soc India. Geological Society of India, Bangalore. 406p

Stampfli GM, Borel GD (2002) A plate tectonic model for the Paleozoic and Mesozoic constrained by dynamic plate boundaries and restored synthetic oceanic isochrons. Earth Planet Sci Lett 196(1):17–33. https://doi.org/10.1016/S0012-821X(01)00588-X

Stübner K, Grujic D, Dunkl I, Thiede R, Eugster P (2018) Pliocene episodic exhumation and the significance of the Munsiari thrust in the northwestern Himalaya. Earth Planet Sci Lett 481:273–283

Tandon SK (1991) The Himalayan foreland: focus on Siwalik basin. In: Tandon SK, Pant CC, Casshyap SM (eds) Sedimentary basins of India. Gyanodaya Prakashk, Nainital, pp 171–201

Tapponier P, Peltzer G, Le Dain AY, Armijo R, Cobbing P (1982) Propagating extrusion tectonics in Asia: new insight from simple experiments with plasticene. Geology 10:69–616

Thakur VC (1993) Geology of the Western Himalaya. Pergamon Press, Oxford. 355p

Thiede RC, Ehlers TA (2013) Large spatial and temporal variations in Himalayan denudation. Earth Planet Sci Lett 371–372:278–293

Thiede RC, Ehlers TA, Bookhagen B, Strecker MR (2009) Erosional variability along the northwest Himalaya. J Geophys Res 114:F1. https://doi.org/10.1029/2008JF001010

Valdiya KS (1980) Geology of the Kumuan Lesser Himalaya. Wadia Inst Himalayan Geol, Dehradun, p 291p

Valdiya KS (2016) The making of India geodynamic evolution. Springer, Switzerland, p 924p

van Hinsbergen DJJ, Lippert PC, Dupont-Nivet G, McQuarrie N, Doubrovine PV, Spakman W, Torsvik TH (2012) Greater India Basin hypothesis and a two-stage Cenozoic collision between India and Asia. Proc Natl Acad Sci U S A 109:7659–7664

Webb AAG, An Y, Harrison TM, Julien C, Burgess WP (2007) The leading edge of the Greater Himalayan Crystalline complex revealed in the NW Indian Himalaya: Implications for the evolution of the Himalayan orogen. Geology 35:955–958. https://doi.org/10.1130/G23931A.1

Webb AAG, Guo H, Clift PD, Husson L, Müller T, Costantino D, Yin A, Xu ZC, Qin W (2017) The Himalaya in 3D: slab dynamics controlled mountain building and monsoon intensification. Lithosphere 9:L636.1. https://doi.org/10.1130/L636.1

Winslow DM, Zeitler PK, Chamberlain CP, Williams IS (1996) Geochronologic constraints on syntaxial development in the Nanga Parbat region, Pakistan. Tectonics 15:1292–1308

Yin A (2006) Cenozoic tectonic evolution of the Himalayan orogen as constrained by along-strike variation of structural geometry, exhumation history, and foreland sedimentation. Earth Sci Rev 76:1–31

Zhao W, Nelson KD, Project INDEPTH Team (1993) Deep seismic reflection evidence for continental underthrusting beneath southern Tibet. Nature 302:557–559